

Reaction of Carbodiphosphorane $\text{Ph}_3\text{P}=\text{C}=\text{PPh}_3$ with $\text{Ni}(\text{CO})_4$. Experimental and Theoretical Study of the Structures and Properties of $(\text{CO})_3\text{NiC}(\text{PPh}_3)_2$ and $(\text{CO})_2\text{NiC}(\text{PPh}_3)_2$

Wolfgang Petz,* Frank Weller, Jamal Uddin, and Gernot Frenking*

Fachbereich Chemie der Universität Marburg, Hans-Meerweinstrasse,
35032 Marburg, Germany

Received June 5, 1998

The carbodiphosphorane $\text{Ph}_3\text{P}=\text{C}=\text{PPh}_3$ (**1**) readily reacts with $\text{Ni}(\text{CO})_4$ in toluene to give the substitution product $(\text{CO})_3\text{NiC}(\text{PPh}_3)_2$ (**2**). If the reaction is carried out in THF solution, additionally red crystals of the dicarbonyl complex $(\text{CO})_2\text{NiC}(\text{PPh}_3)_2$ (**3**) are formed. **2** smoothly converts into **3** when dissolved in THF. The compounds have been characterized by single-crystal X-ray diffraction. Quantum chemical calculations at the DFT level of theory (B3LYP) are given for the geometries of model compounds **1a–3a** with PH_3 ligands instead of PPh_3 , which are in good agreement with the experimental results for **1–3**. The metal–ligand bond energies are also predicted at B3LYP. The calculated $\text{Ni–C}(\text{PH}_3)_2$ bond energy of **3a** ($D_0 = 33.7$ kcal/mol) is nearly the sum of the $\text{Ni–C}(\text{PH}_3)_2$ ($D_0 = 20.9$ kcal/mol) and first Ni–CO bond energy of **2a** ($D_0 = 16.3$ kcal/mol). The analysis of the metal–ligand bonding using the CDA method shows that there is mainly ligand \rightarrow metal donation and much less metal \rightarrow ligand back-donation between Ni and $\text{C}(\text{PH}_3)_2$ in **2a**. Donation and back-donation become stronger and back-donation becomes more important in **3a** than in **2a**.

Introduction

Carbodiphosphoranes, $\text{R}_3\text{P}=\text{C}=\text{PR}_3$, are of considerable interest because of their versatile physical and chemical properties. These double ylides are known with linear¹ or bent^{2–4} structures, depending on the nature of the group R. However, the structures are not rigid and the energy differences between linear and bent forms are probably very small. Similar behavior is reported for the isoelectronic cation $[\text{Ph}_3\text{P}=\text{N}=\text{PPh}_3]^+$ with P–N–P angles ranging between 135° and 180° as the anion is changed.⁵ The crystal structure of $\text{Ph}_3\text{P}=\text{C}=\text{PPh}_3$ (**1**) shows two types of molecules in the unit cell differing in the P–C–P angles by about 14°.² Also structural differences between triboluminescent and nontriboluminescent crystals of **1** exist.³

The bent structure of **1** suggests nucleophilic properties, and the application as ligand for transition metals has been studied by various groups; the organic chem-

istry has been reviewed by Bestmann.⁶ More than 20 years ago Kaska and co-workers described the preparation of the carbonyl derivatives $(\text{CO})_3\text{NiC}(\text{PPh}_3)_2$ ⁷ and $(\text{CO})_5\text{WC}(\text{PPh}_3)_2$,⁸ which are the first and only compounds with **1** coordinated to zerovalent transition metals; however, no structural details were reported. Later, complexes of **1** with higher valent transition metals were presented such as $\text{ClM}(\text{C}(\text{PPh}_3)_2)$ ($\text{M} = \text{Ag}, \text{Cu}$), $(\eta^5\text{-C}_5\text{Me}_5)\text{CuC}(\text{PPh}_3)_2$,⁹ and the ionic species $[\text{O}_3\text{ReC}(\text{PPh}_3)_2]^-$,¹⁰ which have also been studied by X-ray structure analysis.

The chemistry of **1** toward transition metal carbonyl compounds is apparently governed by two main routes as depicted in Scheme 1. In pathway A a CO group is replaced, while the Wittig-type pathway B generates heteroallene-like compounds initiated by a nucleophilic attack of **1** at a carbonyl carbon atom.^{7,8}

In the course of our studies concerning the reactions of $\text{Fe}(\text{CO})_5$ and $(\text{CO})_4\text{FeCS}$ with ylides and various hard and soft nucleophilic species we have also tested the reactivity of **1**. In the case of $\text{Fe}(\text{CO})_5$, even under various reaction conditions, we have not been able to isolate the related $(\text{CO})_4\text{FeC}(\text{PPh}_3)_2$ complex; instead we observed the formation of the Wittig products $(\text{CO})_4\text{Fe}=\text{C}(\text{PPh}_3)_2$.

(6) For the chemistry of **1** see: (a) Bestmann, H. J. *Angew. Chem.* **1977**, *89*, 361; *Angew. Chem., Int. Ed. Engl.* **1977**, *16*, 349. See also recent reviews concerning similar ylides and phosphinocarbenes: (b) Kaska, W. C.; Starzewski, K. A. O. *Ylides and Imines of Phosphorus*; Johnson, W. A., Ed.; John Wiley & Sons: New York, 1993. (c) Bertrand, G. *Coord. Chem. Rev.* **1994**, *137*, 323.

(7) Kaska, W. C.; Mitchell, D. K.; Reichelderfer, R. F.; Korte, W. D. *J. Am. Chem. Soc.* **1974**, *96*, 2847.

(8) Kaska, W. C.; Mitchell D. K.; Reichelderfer, R. F. *J. Organomet. Chem.* **1973**, *47*, 391.

(9) Zybilla, C.; Müller, G. *Organometallics* **1987**, *6*, 2489.

* To whom correspondence should be addressed. E-mail: petz@mailer.uni-marburg.de and frenking@chemie.uni-marburg.de.

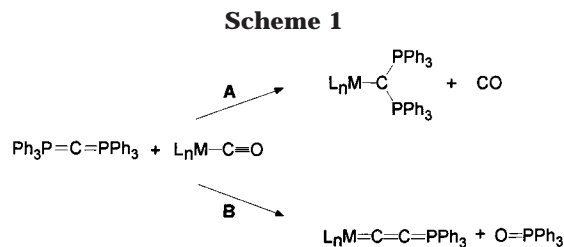
(1) Appel, R.; Baumeister, U.; Knoch, F. *Chem. Ber.* **1983**, *116* (6), 2275.

(2) Vincent, A. T.; Wheatley, P. J. *J. Chem. Soc., Dalton Trans.* **1972**, 617.

(3) Hardy, G. E.; Zink, J. I.; Kaska, W. C.; Baldwin, J. C. *J. Am. Chem. Soc.* **1978**, *100*, 8001.

(4) Ebsworth, E. A. V.; Fraser, T. E.; Rankin, D. W. H.; Gasser, O.; Schmidbaur, H. *Chem. Ber.* **1977**, *110*, 3508.

(5) (a) Handy, L. P.; Ruff, J. K.; Dahl, L. F. *J. Am. Chem. Soc.* **1970**, *92*, 7312. (b) Handy, L. P.; Ruff, J. K.; Dahl, L. F. *J. Am. Chem. Soc.* **1970**, *92*, 7312. (c) Ruff, J. K.; White, R. P.; Dahl, L. F. *J. Am. Chem. Soc.* **1971**, *93*, 2159. (d) Smith, M. B.; Bau, R. *J. Am. Chem. Soc.* **1973**, *95*, 2388. (e) Goldfield, S. A.; Raymond, K. N. *Inorg. Chem.* **1974**, *13*, 770. (f) Chin, H. B.; Smith, M. B.; Wilson, R. D.; Bau, R. *J. Am. Chem. Soc.* **1974**, *96*, 5285. (g) Wilson, R. D.; Bau, R. *J. Am. Chem. Soc.* **1974**, *96*, 7601.

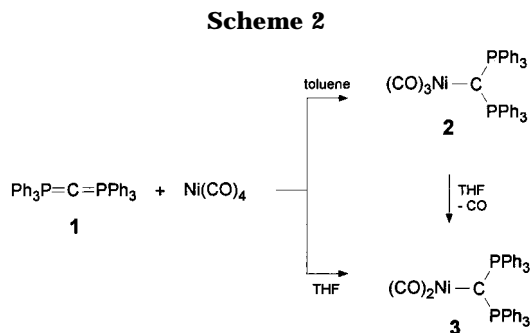


$\text{C}=\text{C}=\text{PPh}_3$ and $\text{Fe}_3(\text{CO})_9(\mu_3-\eta^2-\text{C}\equiv\text{C}\text{PPh}_3)$, following pathway B;¹¹ the thiocarbonyl derivative gives a yellow adduct at low temperature which rapidly decomposes on warming to room temperature producing only tarry materials. The different behavior of **1** toward iron and nickel carbonyls prompted us to look again at the reaction with $\text{Ni}(\text{CO})_4$. We report here about new results concerning this old reaction including spectroscopic information and present the first X-ray structure analyses of nickel carbodiphosphorane complexes. We also present the results of quantum chemical investigations using gradient-corrected density functional theory (B3LYP) of the structures and bonding situation of **1–3** with PH_3 ligands instead of PPh_3 . The metal–ligand bond energies of $\text{Ni}(\text{CO})_n$ ($n = 1–4$) have been calculated for comparison at B3LYP and using coupled-cluster theory¹² at the CCSD(T) level.¹³ The analysis of the bonding situation was carried out with the help of the NBO method¹⁴ and the CDA partitioning scheme.¹⁵ A short outline of the CDA method is given in the Theoretical methods section. More details about the method and a discussion of the application and results can be found in the literature.¹⁶

Results and Discussion

In contrast to the literature report⁷ the reaction of **1** with $\text{Ni}(\text{CO})_4$ produces not only one single product. In toluene as solvent one CO group is replaced to produce exclusively $(\text{CO})_3\text{NiC}(\text{PPh}_3)_2$ (**2**) as large yellow-orange crystals in good yields in agreement with the results of Kaska. However, if the reaction is carried out in THF under the same reaction conditions, deep red crystals are additionally formed along with **2**. To our surprise, the red compound differs from **2** only by loss of one CO group, and the X-ray analysis confirms the monomeric formula $(\text{CO})_2\text{NiC}(\text{PPh}_3)_2$ (**3**) in which the Ni atom attains coordination number 3 with 16 instead of 18 valence electrons (Scheme 2).

2 can be transformed into **3** by dissolving in THF. In contrast to the results with $\text{Fe}(\text{CO})_5$, the related Wittig



product $(\text{CO})_3\text{Ni}=\text{C}=\text{C}=\text{PPh}_3$ according to pathway B could not be detected. Although coordination number 3 and formation of 16 valence electron compounds is very common in Ni(0) chemistry, to our knowledge, **3** is the first complex in which the $(\text{CO})_2\text{Ni}$ fragment is bonded to only one further donor ligand, generating a three-coordinate electron-deficient nickel atom.¹⁷

The relatively weak bond of **1** to the Ni atom is documented by reacting the compounds with better π acceptor ligands such as phosphines. Thus, a mixture of **2** and **3** in THF solution reacts even at -78°C with PPh_3 , liberating quantitatively the carbodiphosphorane to give a mixture of $(\text{CO})_3\text{NiPPh}_3$ and $(\text{CO})_2\text{Ni}(\text{PPh}_3)_2$; both compounds were identified by their characteristic IR and ³¹P NMR data.



The spectroscopic data for **2** and **3** are consistent with the structures proposed. The IR spectrum of **2** exhibits the typical pattern of a $\text{Ni}(\text{CO})_3$ group with local C_{3v} symmetry. A sharp band at 2032 cm^{-1} and a broad band at 1933 cm^{-1} correspond to the symmetrical (A_1) and antisymmetrical (E) $\nu(\text{CO})$ vibrations, respectively. Two sharp and intense vibrations at 1976 cm^{-1} (A_1) and 1895 cm^{-1} (B_1) in the spectrum of **3** are typical for a $\text{Ni}(\text{CO})_2$ group. However, the center of the bands is shifted to lower frequencies relative to that of related $(\text{CO})_2\text{Ni}(\text{PR}_3)_2$ compounds,¹⁷ but comparable with the shift found in a $(\text{CO})_2\text{Ni}(\text{carbene})_2$ compound.¹⁸ This indicates that the presence of **1** at the Ni atom induces a strong back-donation of negative charge into the CO π^* orbitals comparable to the action of two nucleophilic carbene ligands of the Arduengo type.¹⁸

To get more insight into the properties of the compounds for further chemical reactions, the molecular structures of **2** and **3** have been determined by single-crystal X-ray diffraction studies. Suitable crystals were grown from toluene and THF solutions, respectively, by layering with pentane. ORTEP views of the molecules are presented in Figures 1 and 2. A special view of the core of **3** is shown in Figure 3. Selected bond distances and angles are collected in Tables 1 and 2.

The geometry of **2** at the Ni atom is that of a nearly ideal tetrahedron, with angles ranging between 105° and 113° , consistent with a 18-electron configuration.

(10) Sundermeyer, J.; Weber, K.; Peters, K.; von Schnering, H. G. *Organometallics* **1994**, *13*, 2560.

(11) Petz, W.; Weller, F. Z. *Naturforsch.* **1996**, *51b*, 1598.

(12) (a) Cizek, J. *J. Chem. Phys.* **1966**, *45*, 4256. (b) Cizek, J. *Adv. Chem. Phys.* **1966**, *14*, 35.

(13) (a) Pople, J. A.; Krishnan, R.; Schlegel, H. B.; Binkley, J. S. *Int. J. Quantum Chem.* **1978**, *14*, 545. (b) Bartlett, R. J.; Purvis, G. D. *Ibid.* **1978**, *14*, 561. (c) Purvis, G. D.; Bartlett, R. J. *J. Chem. Phys.* **1982**, *76*, 1910. (d) Purvis, G. D.; Bartlett, R. J. *Ibid.* **1987**, *86*, 7041.

(14) Reed, A. E.; Curtiss, L. A.; Weinhold, F. *Chem. Rev.* **1988**, *88*, 899.

(15) Dapprich, S.; Frenking, G. *J. Phys. Chem.* **1995**, *99*, 9352.

(16) (a) Frenking, G.; Pidun, U. *J. Chem. Soc., Dalton Trans.* **1997**, 1653. (b) Pidun, U.; Frenking, G. *J. Organomet. Chem.* **1996**, *525*, 269. (c) Pidun, U.; Frenking, G. *Organometallics* **1995**, *14*, 5325. (d) Ehlers, A. W.; Dapprich, S.; Vyboshchikov, S. F.; Frenking, G. *Organometallics* **1996**, *15*, 105. (e) Dapprich, S.; Frenking, G. *Organometallics* **1996**, *15*, 4547. (f) Frenking, G.; Dapprich, S.; Köhler, K. F.; Koch, W.; Collins, J. R. *Mol. Phys.* **1996**, *89*, 1245.

(17) (a) *Gmelin Handbuch der Anorganischen Chemie*; Springer-Verlag: Berlin, 1975; Nickel-Organische Verbindungen Teil 1. (b) *Gmelin Handbook of Inorganic and Organometallic Chemistry*; Springer-Verlag: Berlin, 1996; Organonickel Compounds Suppl. Vol. 3.

(18) Two $\nu(\text{CO})$ vibrations are observed at 1946 and 1873 cm^{-1} : Öfele, K.; Herrmann, W. A.; Mihalios, D.; Elison, M.; Herdtweck, E.; Scherer, W.; Mink, J. *J. Organomet. Chem.* **1993**, *459*, 177.

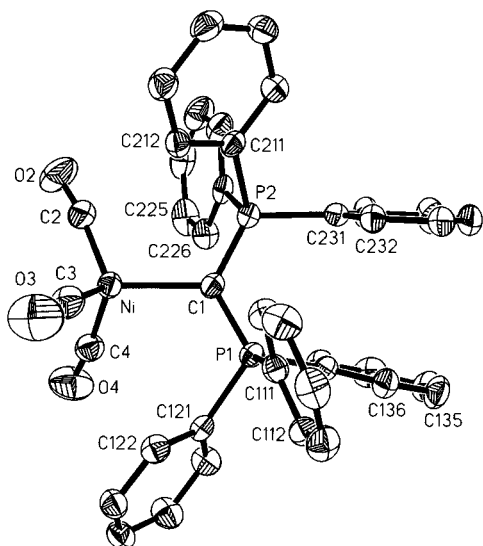


Figure 1. Molecular structure of $(\text{CO})_3\text{NiC}(\text{PPh}_3)_2$ (**2**). Hydrogen atoms are omitted for clarity.

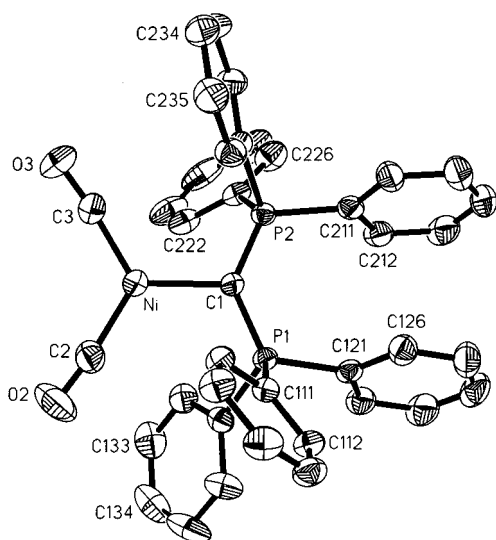


Figure 2. Molecular structure of $(\text{CO})_2\text{NiC}(\text{PPh}_3)_2$ (**3**). Hydrogen atoms are omitted for clarity.

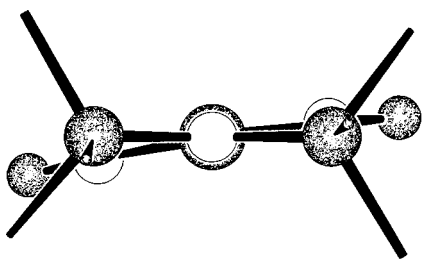


Figure 3. View down the $\text{C}(1)\text{-Ni}$ axis in **3**.

The sum of the angles at $\text{C}(1)$ amounts to 360° , indicating planarity. The dative bond from the ligand to Ni yields a bond separation of 211.0 pm, which is the longest one found for a Ni-C bond length. To our knowledge, only two crystal structure studies of compounds are available in which the $(\text{CO})_3\text{Ni}$ fragment is bonded to a carbon donor ligand. These are the ylide complex $(\text{CO})_3\text{NiCH}(\text{Me})=\text{PCy}_3$, with a Ni-C bond length of 209.6 pm,¹⁹ and the Arduengo type carbene

Table 1. Experimental Data for the X-ray Diffraction Studies of Complexes **2** and **3**

	2	3
formula	$\text{C}_{40}\text{H}_{30}\text{NiO}_3\text{P}$	$\text{C}_{39}\text{H}_{30}\text{NiO}_3\text{P}$
mw	679.29	651.28
crystal system	monoclinic	triclinic
space group	$P2(1)/c$	$P\bar{1}$
a (pm)	1635.3(3)	1100.89(17)
b (pm)	1133.94(14)	1241.3(3)
c (pm)	1903.7(3)	1318.5(3)
α (deg)	90	89.771(18)
β (deg)	109.978(11)	78.547(11)
γ (deg)	90	68.087(11)
volume (\AA^3)	3317.7(8)	1633.4(5)
Z	4	2
d_{calcd} (g/cm^3)	1.360	1.324
abs coeff (mm^{-1})	0.719	0.725
$F(000)$	1408	676
crystal size (mm)	$0.18 \times 0.23 \times 0.41$	$0.15 \times 0.27 \times 0.37$
temp (K)	293(2)	293(2)
θ range for data collection (deg)	2.13–24.99	1.77–24.00
index range	$-1 \leq h \leq 19, -1 \leq k \leq 13, -1 \leq l \leq 18$	$-12 \leq h \leq 0, -14 \leq k \leq 13, -15 \leq l \leq 14$
no. of reflns collected/unique completeness to $2\theta = 24.99$	6786/5558 [$R(\text{int}) = 0.0289$]	5381/5079 [$R(\text{int}) = 0.0677$]
refinement method	full-matrix least-squares on F^2	full-matrix least-squares on F^2
no. of data/restraints/params	5558/0/349	5079/0/331
goodness-of-fit on F^2	1.013	1.021
final R indices [$I < 2\sigma(I)$]	$R1 = 0.0432,$ $wR2 = 0.0974$	$R1 = 0.0378,$ $wR2 = 0.0882$
R indices (all data)	$R1 = 0.0658,$ $wR2 = 0.1079$	$R1 = 0.0481,$ $wR2 = 0.0928$
largest diff peak and hole (e \AA^{-3})	0.360 and -0.367	0.386 and -0.309

^a Sheldrick, G. M. *SHELXTL-Plus*, Release 4.0 for R3 Crystallographic Research Systems; Siemens Analytical X-ray Instruments Inc.: Madison, WI, 1989. ^b Spek, A. L. *Platon-89*; University of Utrecht, 1989. ^c Keller, E. *Schakal-86*, A FORTRAN Program for the Graphical Presentation of Molecular and Crystallographic Models; Freiburg, 1989. ^d Sheldrick, G. M. *SHELXL-93*; Universität Göttingen, 1993. ^e International Tables 1974.

Table 2. Selected Distances and Angles in $(\text{CO})_3\text{NiC}(\text{PPh}_3)_2$ (**2**) and $(\text{CO})_2\text{NiC}(\text{PPh}_3)_2$ (**3**)

	2	3
Distances (pm)		
$\text{Ni}(1)\text{-C}(3)$	178.2(4)	$\text{Ni}(1)\text{-C}(3)$ 174.0(3)
$\text{Ni}(1)\text{-C}(2)$	178.6(4)	$\text{Ni}(1)\text{-C}(2)$ 175.2(3)
$\text{Ni}(1)\text{-C}(4)$	179.2(4)	
$\text{Ni}(1)\text{-C}(1)$	211.0(3)	$\text{Ni}(1)\text{-C}(1)$ 199.0(3)
$\text{P}(1)\text{-C}(1)$	168.1(3)	$\text{P}(1)\text{-C}(1)$ 167.7(3)
$\text{P}(1)\text{-C}(121)$	183.42(16)	$\text{P}(1)\text{-C}(121)$ 183.82(14)
$\text{P}(1)\text{-C}(131)$	183.90(16)	$\text{P}(1)\text{-C}(131)$ 184.11(15)
$\text{P}(1)\text{-C}(111)$	184.41(15)	$\text{P}(1)\text{-C}(111)$ 184.40(13)
$\text{P}(2)\text{-C}(1)$	167.4(3)	$\text{P}(2)\text{-C}(1)$ 167.6(3)
$\text{P}(2)\text{-C}(231)$	183.11(16)	$\text{P}(2)\text{-C}(231)$ 183.37(14)
$\text{P}(1)\text{-C}(221)$	183.28(16)	$\text{P}(1)\text{-C}(221)$ 183.47(14)
$\text{P}(1)\text{-C}(211)$	185.47(16)	$\text{P}(1)\text{-C}(211)$ 184.83(14)
$\text{C}(2)\text{-O}(2)$	114.0(4)	$\text{C}(2)\text{-O}(2)$ 114.4(4)
$\text{C}(3)\text{-O}(3)$	113.0(4)	$\text{C}(3)\text{-O}(3)$ 115.1(3)
$\text{C}(4)\text{-O}(4)$	113.5(4)	
Angles (deg)		
$\text{C}(3)\text{-Ni}(1)\text{-C}(2)$	113.23(16)	$\text{C}(3)\text{-Ni}(1)\text{-C}(2)$ 118.02(14)
$\text{C}(3)\text{-Ni}(1)\text{-C}(4)$	107.71(17)	
$\text{C}(2)\text{-Ni}(1)\text{-C}(4)$	104.95(16)	
$\text{C}(3)\text{-Ni}(1)\text{-C}(1)$	110.43(15)	$\text{C}(3)\text{-Ni}(1)\text{-C}(1)$ 120.96(12)
$\text{C}(2)\text{-Ni}(1)\text{-C}(1)$	112.59(14)	$\text{C}(2)\text{-Ni}(1)\text{-C}(1)$ 120.90(12)
$\text{C}(4)\text{-Ni}(1)\text{-C}(1)$	107.52(14)	
$\text{P}(1)\text{-C}(1)\text{-P}(2)$	124.58(19)	$\text{P}(1)\text{-C}(1)\text{-P}(2)$ 132.13(16)
$\text{P}(1)\text{-C}(1)\text{-Ni}(1)$	120.25(17)	$\text{P}(1)\text{-C}(1)\text{-Ni}(1)$ 112.81(13)
$\text{P}(2)\text{-C}(1)\text{-Ni}(1)$	115.16(16)	$\text{P}(2)\text{-C}(1)\text{-Ni}(1)$ 115.06(13)

complex $(\text{CO})_3\text{NiCN}(\text{R})\text{CH}=\text{CHNR}$ ($\text{R} = \text{CHMePh}$), in which a separation of 198.6 pm was measured.²⁰

(19) Barnett, B. L.; Krüger, C. *J. Cryst. Mol. Struct.* **1972**, *2*, 271.

Table 3. Comparison of Related Bonding Parameters of 1–3 and the Ylide Complex (CO)₃NiCH(Me)=PCy₃ (4)

complex	Ni–C(P) (pm)	P–C(ylide) (pm)	Ni–C(O) (pm)	P–C–P (deg)	ref
1		163.3 (I), 162.9 (II)		130.1 (I), 143.8 (II)	2 ^a
1		161.0		134.4	3 ^b
2	211.0	167.3	178.7	124.6	this work
3	199.0	167.6	174.6	132.1	this work
4	209.6	174.5	175		19

^a Triboluminescent crystals, molecules I and II. ^b Nontriboluminescent crystals.

The short P–C bonds and the very long Ni–C bond lead to the conclusion that the carbodiphosphorane ligand in **2** acts as a pure σ donor with P–C double bonds, while a carbene-like Ni–C double bond plays no significant role.

The loss of one CO group in going from **2** to **3** induces a variety of interesting changes in bond parameters, as depicted in Table 3. The most dramatic change is the shortening of the Ni–C separation by 12 pm, indicating an appreciable increase in bond order. Additionally the P–C–P bond angle opens from 124° in **2** to 132° in **3**. The Ni atom of **3** lies in a trigonal planar environment with approximately 120° angles at the Ni center ($\Sigma = 359.9(1)^\circ$). As in **2** the donating carbon atom C(1) is exactly sp^2 hybridized ($\Sigma = 360.0(1)^\circ$) with angles varying between 115° and 132°. The C–Ni–C plane forms a dihedral angle with the plane spanned by the P–C–P atoms of only 9.3°. Nearly 10 atoms including the ipso carbon atoms of two phenyl groups are located approximately in one plane. The relatively short Ni–C distance and the nearly planar ligand arrangement forms an “ethene”-like molecule core; a view down the carbodiphosphorane C–Ni bond is shown in Figure 3. The small deviation by 9° from ideal planarity is probably due to packing effects and not electronic in nature.

Calculations on the model system **3a**, which are described in detail below, show that loss of one CO group on going from **2** to **3** increases the σ donor properties of the ligand and also the π back-donation from metal d orbitals to all the ligands; the compound however remains a 16-electron species. An alternative function of the carbodiphosphorane as a four-electron donor as in highly oxidized systems¹⁰ can be excluded.

A shorter Ni–C bond as in **3** is found in the 16-electron diolefin carbene complex (CH₂=CH₂)₂Ni=C(Ph)-NMeBu-t with 188.9 pm;²¹ the shortest Ni–C bond with 183.0 pm was reported by Arduengo et al. to be operative in the linear biscarbene complex R₂C=Ni=CR₂ containing the 1,3-dimesitylimidazol-2-ylidene ligand R₂C.²²

The change of geometry at Ni on going from **2** to **3** is also accompanied by a shortening of the Ni–C bond distances to the carbonyl groups by about 4.5 pm, indicating an increase in Ni → CO π back-donation being in line with the low-frequency $\nu(\text{CO})$ vibration

found in the IR spectrum. On the other hand, the P–C(ylide) bond distances in **2** and **3** are nearly equal but are shorter (167 pm) than those in the anion [O₃ReC(PPh₃)₂][−], where a strong Re–C double bond is suggested, causing an elongation of the P–C(ylide) bond distances to 177 pm.¹⁰

In both compounds a perfectly planar donor center is operative, with the angles at the donating carbon atom summing up to 360°. A nearly parallel arrangement of two phenyl rings is found in the free ligand as well as in the versatile complexes.

A comparison of the chemistry of **1** toward various transition metal carbonyl compounds reveals some interesting questions. Why does the carbodiphosphorane react so differently with Fe(CO)₅ and Ni(CO)₄?

The results show that the carbodiphosphorane molecule can be considered first as a “hard” Lewis base, which preferentially attacks an electrophilic carbonyl carbon atom. In the bent structure the carbon p orbital is not empty as in the related carbene ligands, which makes **1** not very attractive for low-valent transition metal fragments. In Ni(CO)₄ the carbonyl carbon atoms are probably less electrophilic than in Fe(CO)₅, because more d electrons form back-bonds to fewer CO molecules. On the other hand the first carbonyl dissociation energy is less for Ni(CO)₄ (calc 29.9, expt 25 kcal/mol) than for Fe(CO)₅ (calc 45.7,²³ expt 42 kcal/mol), which is probably the most important reason for preferring CO substitution over nucleophilic attack at the carbon atom in the nickel complex.^{23,24}

Theoretical Studies

We optimized the geometries of the model compounds C(PH₃)₂ (**1a**), (CO)₃NiC(PH₃)₂ (**2a**), and (CO)₂NiC(PH₃)₂ (**3a**) at the B3LYP/II level of theory. The Ni–CO and Ni–C(PH₃)₂ bond energies were also calculated at B3LYP/II. We present also for comparison calculated results of Ni(CO)_n ($n = 1-4$) at B3LYP/II and CCSD(T)/II using B3LYP/II optimized geometries.

The excellent agreement of the calculated geometries of the model compounds **1a–3a** shown in Figure 4 with the experimentally derived structures of **1–3** given in Table 3 justifies the use of PH₃ for PPh₃ in the model compounds. **1a** has a bent structure with a calculated P–C–P bond angle of 138.1°. The experimentally reported P–C–P angle for **1** is 130.1–143.8°.^{2,3} The P–C–P bond angle becomes more acute in **2a** (124.6°) and slightly less acute in **3a** (126.6°). This is in agreement with the trend of the experimental values for **2** and **3**, although the opening of the bond angle from **2** to **3** (124° to 132°) is larger than it is calculated for **2a** and **3a**. The Ni–C(PH₃)₂ and Ni–CO bond lengths in **3a** (Ni–C(PH₃)₂ 197.7 pm; Ni–CO 176.8 pm) are significantly shorter than in **2a** (Ni–C(PH₃)₂ 209.0 pm; Ni–CO 181.0 pm), which conforms with the experimental values for **2** and **3**. The C–PH₃ bond lengths in the complexes **2a** (167.0 pm) and **3a** (166.8 pm) are nearly the same. They are slightly longer than in free **1a** (163.1

(20) Herrmann, W. A.; Goossen, L. J.; Artus, G. R. L.; Köcher, C. *Organometallics* **1997**, *16*, 2472.

(21) Gabor, B.; Krüger, C.; Marczinke, B.; Mynott, R.; Wilke, G. *Angew. Chem.* **1991**, *103*, 1711; *Angew. Chem., Int. Ed. Engl.* **1991**, *30*, 1666.

(22) Arduengo, A. J., III; Gamper, S. F.; Calabrese, J. C.; Davidson, F. *J. Am. Chem. Soc.* **1994**, *116*, 4391.

(23) (a) Li, J.; Schreckenbach, J.; Ziegler, T. *J. Am. Chem. Soc.* **1995**, *117*, 486. (b) Ziegler, T.; Tschinke, V.; Ursenbach, C. *J. Am. Chem. Soc.* **1987**, *109*, 4825, and literature therein. See also: Angelici, R. J. *Acc. Chem. Res.* **1972**, *5*, 335.

(24) Delley, B.; Wrinn, M.; Lüthi, H. P. *J. Chem. Phys.* **1994**, *100*, 5785.

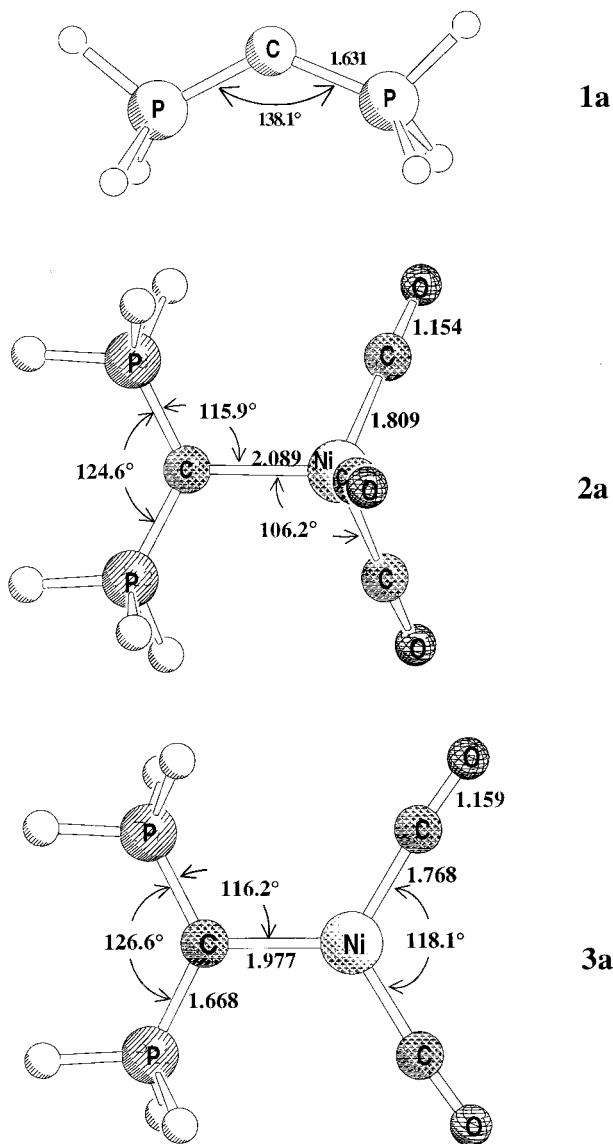


Figure 4. Calculated structures of the model compounds **1a–3a** at B3LYP/II. Bond lengths in angstroms, angles in degree.

pm). Again, this is in agreement with the experimental results for **1–3**.

The observation that **2** and **3** are formed together during the reaction of **1** with $\text{Ni}(\text{CO})_4$ suggests that the Ni–C(PPh_3)₂ bond energy of **3** should be roughly the sum of the Ni–C(PPh_3)₂ and first Ni–CO bond dissociation energies of **2**. We calculated the Ni–C(PPh_3)₂ and Ni–CO bond energies of **2a** and **3a** at B3LYP/II and the Ni–CO bond energies of $\text{Ni}(\text{CO})_4$ at B3LYP/II and CCSD(T)/II. The results are shown in Table 4. The calculated metal–ligand bond energies of **2a** at B3LYP/II are $D_0 = 20.9$ kcal/mol for Ni–C(PPh_3)₂ and $D_0 = 16.3$ kcal/mol for Ni–CO. The Ni–C(PPh_3)₂ bond energy of **3a**, $D_0 = 33.7$ kcal/mol, is clearly higher compared with **2a**, and it is indeed nearly the sum of the Ni–C(PPh_3)₂ and Ni–CO bond energies of **2a** (37.2 kcal/mol). The theoretically predicted bond energies at B3LYP/II indicate that the Ni–C(PPh_3)₂ bonds in **2a** and **3a** are stronger than the Ni–CO bonds in $\text{Ni}(\text{CO})_4$ and $\text{Ni}(\text{CO})_3$, respectively.

The accuracy of the theoretically predicted binding energies, which were calculated with rather modest

basis sets, may be estimated by comparing the theoretical bond energies for $\text{Ni}(\text{CO})_n$ at B3LYP/II and CCSD(T)/II with experimental values^{25,26} and with a previous theoretical study at the CCSD(T) level using larger all-electron basis sets than in our work.²⁷ Table 4 shows that the CCSD(T)/II values are in good agreement with the experimental values, except for $\text{Ni}(\text{CO})_2$, where the theoretical bond energy is too low. However, CCSD(T) calculations with a larger basis set²⁷ and CASPT2 calculations²⁸ give similar bond energies for $\text{Ni}(\text{CO})_2$, as predicted at CCSD(T)/II. It seems possible that the experimental value for the bond energy of $\text{Ni}(\text{CO})_2$ is too high. The B3LYP/II bond energies are similar to the CCSD(T)/II values, with the exception of $\text{Ni}(\text{CO})$. It has been shown that DFT methods have problems with transition metal monocarbonyls.²⁹

Generally, the CCSD(T) calculations with the moderate basis set II are in good agreement with experimental results, which is due to a fortuitous error cancellation of BSSE effects and insufficient description of the bonding region. This seems to be a general effect of this level of theory. Previous calculations have shown that the first dissociation energies of transition metal carbonyls predicted at CCSD(T)/II are in very good agreement (± 3 kcal/mol) with experimental results.^{31,32} Partial cancellation of BSSE effects and basis set incompleteness error has also been noticed for DFT calculations.⁴⁹

Table 5 shows the calculated C–O stretching frequencies of $\text{Ni}(\text{CO})_n$ **2a** and **3a** together with the experimental values for the nickel carbonyls **2** and **3**. Please note that the calculated values refer to harmonic frequencies,

(25) Stevens, A. E.; Feigerle, C. S.; Lineberger, W. C. *J. Am. Chem. Soc.* **1982**, *104*, 5026.

(26) Sunderlin, L. S.; Squires, R. R. Private communication, cited in ref 27.

(27) Blomberg, M. R. A.; Siegbahn, P. E. M.; Lee, T. J.; Rendell, A. P.; Rice, J. E. *J. Chem. Phys.* **1991**, *95*, 5898.

(28) Persson, B. J.; Roos, B. O.; Pierloot, K. *J. Chem. Phys.* **1994**, *101*, 6810.

(29) For example, the metal–CO bond energies of the monocarbonyls $\text{Cu}(\text{CO})^+$ and $\text{Ag}(\text{CO})^+$ are predicted at BP86 and B3LYP to be lower than the first bond dissociation energies of the dicarbonyls $\text{Cu}(\text{CO})_2^+$ and $\text{Ag}(\text{CO})_2^+$, respectively. This is in disagreement with experimental evidence and with the results of MP2 and CCSD(T) calculations: Jonas, V.; Lupinetti, A. J.; Frenking, G.; Strauss, S. H.; Thiel, W. *J. Phys. Chem.*, submitted for publication.

(30) Moore, C. E. *Natl. Bur. Stand. Circ.* 467; U.S. GPO: Washington, D.C., 1952.

(31) Frenking, G.; Antes, I.; Böhme, M.; Dapprich, S.; Ehlers, A. W.; Jonas, V.; Neuhaus, A.; Otto, M.; Stegmann, R.; Veldkamp, A.; Vyboishchikov, S. F. In *Reviews in Computational Chemistry*, Vol. 8; Lipkowitz, K. B., Boyd, D. B., Eds.; VCH: New York, 1996; pp 63–144.

(32) (a) Ehlers, A. W.; Frenking, G. *J. Am. Chem. Soc.* **1994**, *116*, 1514. (b) Ehlers, A. W.; Frenking, G. *Organometallics* **1995**, *14*, 423. (c) Ehlers, A. W.; Dapprich, S.; Vyboishchikov, S. F.; Frenking, G. *Organometallics* **1996**, *15*, 105.

(33) (a) DeKock, R. L. *Inorg. Chem.* **1971**, *10*, 1205. (b) Rosen, B. *Spectroscopic Data Related to Diatomic Molecules*; Pergamon Press: Oxford, 1971.

(34) Braterman, P. S. *Metal Carbonyl Spectra*; Academic Press: London, 1975.

(35) Becke, A. D. *J. Chem. Phys.* **1993**, *98*, 5648.

(36) Hay, P. J.; Wadt, W. R. *J. Chem. Phys.* **1985**, *82*, 299.

(37) (a) Ditchfield, R.; Hehre, W. J.; Pople, J. A. *J. Chem. Phys.* **1971**, *54*, 724. (b) Hehre, W. J.; Ditchfield, R.; Pople, J. A. *J. Chem. Phys.* **1972**, *56*, 2257. (c) Hariharan, P. C.; Pople, J. A. *Mol. Phys.* **1974**, *27*, 209. (d) Hariharan, P. C.; Pople, J. A. *Theor. Chim. Acta* **1973**, *28*, 213. (e) Gordon, M. S. *Chem. Phys. Lett.* **1980**, *76*, 163.

(38) Bergner, A.; Dolg, M.; Küchle, W.; Stoll, H.; Preuss, H. *Mol. Phys.* **1993**, *80*, 1431.

(39) Andzelm, J.; Huzinaga, S.; Klobukowski, M.; Radzio, E.; Sakai, Y.; Tatekawa, H. *Gaussian Basis Sets for Molecular Calculations*; Elsevier: Amsterdam, 1984.

Table 4. Calculated and Experimental Binding Energies [kcal/mol] D_e and ZPE-Corrected Values D_0

	B3LYP/II		CCSD(T)/II ^a		CCSD(T) ^d	CASPT2 ^e	expt ^b
	D_e	D_0	D_e	D_0	D_0	D_0	D_0
Ni(CO) → Ni + CO	27.68 ^f	25.98 ^f	43.49 ^f	41.79 ^f	34.5	40.7	35 ± 3
Ni(CO) ₂ → Ni(CO) + CO	46.52	45.02	42.89	41.59	42.6	39.1	51 ± 4
Ni(CO) ₃ → Ni(CO) ₂ + CO	30.76	29.06	32.59	30.90	34.6	27.8	29 ± 2
Ni(CO) ₄ → Ni(CO) ₃ + CO	21.89	19.96	24.50	22.72	29.8	27.9	25 ± 2 ^c
2a → 3a + CO	17.80	16.28					
2a → Ni(CO) ₃ + C(PH ₃) ₂	22.27	20.93					
3a → Ni(CO) ₂ + C(PH ₃) ₂	35.23	33.73					

^a At B3LYP/II optimized geometry, this work. ^b Ref 26. ^c Ref 25. ^d Ref 27. ^e Ref 28. ^f Calculated using the theoretical energy for the ¹S(d¹⁰) state of the Ni atom and the experimental ³D → ¹S excitation energy (1.74 eV).³⁰

Table 5. Calculated and Experimental CO Stretching Frequencies (in cm⁻¹)

	sym	B3LYP/II				experimental			
		$\nu(\text{CO})$		$\Delta\nu(\text{CO})^e$		$\nu(\text{CO})$		$\Delta\nu(\text{CO})^e$	
		sym	as	sym	as	sym	as	sym	as
CO		2211				2143 ^b			
Ni(CO)	$D_{\infty h}$	2099		-112		1996 ^b		-147	
Ni(CO) ₂	C_{2v}	2178	2090	-33	-121	2100 ^a	1967 ^b	-43	-176
Ni(CO) ₃	D_{3h}	2190	2116	-21	-95	2100 ^a	2017 ^b	-43 ± 80	-126
Ni(CO) ₄	T_d	2202	2136	-9	-75	2132 ^c	2058 ^c	-11	-85
2a	C_1	2133	2071	-78	-140	2032 ^d	1933 ^d	-111	-210
3a	C_1	2097	2040	-114	-171	1976 ^d	1895 ^d	-167	-248

^a Ref 25. ^b Ref 33. ^c Ref 34. ^d This work, compounds **2** and **3**. ^e Frequency shift relative to free CO.

while the experimental values refer to anharmonic frequencies. The absolute values of the stretching modes may therefore be different, but the *trend* of the experimental and calculated wavenumbers should run parallel. The data in Table 5 indicate that the calculated and experimentally observed shifts of the C–O stretching mode agree very nicely. The shift of the asymmetric C–O stretching mode is always higher compared to the symmetric mode. We want to point out that theory and experiment indicate that the shift of the C–O frequencies toward smaller wavenumbers for **3** (**3a**) and even more for **2** (**2a**) with respect to free CO is much higher compared to Ni(CO)₄. The frequency shifts suggest that the Ni → CO π back-donation in the carbodiphosphorane complexes is stronger than in Ni(CO)₄. This conclusion is in agreement with the analysis of the metal–ligand interactions given below.

Table 6 shows the calculated charge distribution of the molecules given by the NBO method.¹⁴ The Ni atom always carries a positive partial charge. The positive

Table 6. Calculated NBO Charge Distribution

molecule	Ni	C ^a	C(PH ₃) ₂	CO
Ni(CO)	0.06			-0.06
Ni(CO) ₂	0.05			-0.03
Ni(CO) ₃	0.22			-0.07
Ni(CO) ₄	0.33			-0.08
2a	0.38	-1.62	0.11	-0.16
3a	0.30	-1.67	0.07	-0.19
1a		-1.58	0	

^a Carbon atom of the C(PH₃)₂ ligand.

charge at Ni in **2a** is higher than in Ni(CO)₄. It is also higher in **3a** than in Ni(CO)₃. Since the carbodiphosphorane ligand in **2a** and **3a** also has a small positive partial charge, it follows that the carbonyl ligands in **2a** and **3a** are more negatively charged than in the binary carbonyls. The positive charge of the C(PH₃)₂ groups in **2a** and **3a** suggests that the Ni ← C(PH₃)₂ σ donation might be more important than the Ni → C(PH₃)₂ π back-donation. A more detailed picture about the donor–acceptor interactions is given by the results of the CDA method (Table 7), which has proven to be very helpful for the analysis of donor–acceptor interactions.¹⁶ The CDA results give the amount of ligand → metal charge donation, metal → ligand back-donation, and also the metal ↔ ligand repulsive polarization, which arises from the mixing of the occupied orbitals of the ligand and the metal fragment. This term is negative, because electronic charge is removed from the overlapping area of the occupied orbitals.

The data in Table 7 show that the C(PH₃)₂ ligand in the complex **2a** is a much stronger electron donor than electron acceptor. The donation/back-donation (d/b) ratio is 4.93. This may be compared with the d/b ratio of 2.11 for CO in Ni(CO)₄. Carbon monoxide becomes a slightly better acceptor in **2a**, which has a d/b ratio for CO of 1.79. The carbodiphosphorane ligand and CO become slightly better electron acceptors in the complex **3a**, which has a d/b ratio of 3.45 for C(PH₃)₂ and 1.71 for CO. The CDA results are in agreement with the conclusions that have been made from the chemical behavior

(40) Frisch, M. J.; Trucks, G. W.; Schlegel, H. B.; Gill, P. M. W.; Johnson, B. G.; Robb, M. A.; Cheeseman, J. R.; Keith, T. A.; Petersson, G. A.; Montgomery, J. A.; Raghavachari, K.; Al-Laham, M. A.; Zakrzewski, V. G.; Ortiz, J. V.; Foresman, J. B.; Cioslowski, J.; Stefanov, B. B.; Nanayakkara, A.; Challacombe, M.; Peng, C. Y.; Ayala, P. Y.; Chen, W.; Wong, M. W.; Andres, J. L.; Replogle, E. S.; Gomberts, R.; Martin, R. L.; Fox, D. J.; Binkley, J. S.; Defrees, D. J.; Baker, I.; Stewart, J. J. P.; Head-Gordon, M.; Gonzalez, C.; Pople, J. A. *Gaussian 94*; Gaussian Inc.: Pittsburgh, PA, 1995.

(41) Stanton, J. F.; Gauss, J.; Watts, J. D.; Lauderdale, W. J.; Bartlett, R. J. *ACES II*, an ab initio program system; University of Florida: Gainesville, FL, 1991.

(42) Werner, H.-J.; Knowles, P. J. Universität Stuttgart and University of Birmingham.

(43) Dapprich, S.; Frenking, G. *CDA 2.1*; Marburg, 1994. The program is available on-line: ftp://chemie.uni-marburg.de/pub/cda).

(44) Ramirez, F.; Desai, N. B.; Hansen, B.; McKelvie, N. *J. Am. Chem. Soc.* **1961**, *83*, 3539.

(45) Davidson, E. R.; Kunze, K. L.; Machado, F. B. C.; Chakravorty, S. *J. Acc. Chem. Res.* **1993**, *26*, 628.

(46) Szilagy, R.; Frenking, G. *Organometallics* **1997**, *16*, 4807.

(47) Herrmann, W. A.; Köcer, C. *Angew. Chem.* **1997**, *109*, 2257; *Angew. Chem., Int. Ed. Engl.* **1997**, *36*, 2162.

(48) Boehme, C.; Frenking, G. *Organometallics* **1998**, *17*, 5801.

(49) Rosa, A.; Ehlers, A. W.; Baerends, E. J.; Snijders, J. G.; te Velde, G. *J. Phys. Chem.* **1996**, *100*, 5690.

Table 7. Results of the Charge Decomposition Analysis of the Complexes: Calculated (B3LYP/II) Donation d (A \rightarrow B), Back-Donation b (A \leftarrow B), Repulsive Polarization r (A \leftrightarrow B), and Residue Term Δ between the Ligand A and the Fragment B in the Complex C

molecule	d	b	d/b	r	Δ
C $(\text{PH}_3)_2\text{C}-\text{Ni}(\text{CO})_3$	0.355	0.072	4.93	-0.238	-0.027
A $\text{C}(\text{PH}_3)_2$					
B $\text{Ni}(\text{CO})_3$					
C $\text{CO}-\text{Ni}(\text{CO})_2\text{C}(\text{PH}_3)_2$	0.482	0.270	1.79	-0.206	-0.009
A $\text{CO}-\text{Ni}(\text{CO})_3$					
B $(\text{CO})_2\text{Ni}-\text{C}(\text{PH}_3)_2$					
C $(\text{PH}_3)_2\text{C}-\text{Ni}(\text{CO})_2$	0.428	0.124	3.45	-0.238	-0.017
A $\text{C}(\text{PH}_3)_2$					
B $\text{Ni}(\text{CO})_2$					
C $\text{CO}-\text{Ni}(\text{CO})\text{C}(\text{PH}_3)_2$	0.505	0.296	1.71	-0.207	-0.006
A CO					
B $\text{Ni}(\text{CO})\text{C}(\text{PH}_3)_2$					
C $\text{CO}-\text{Ni}$	0.499	0.355	1.41	0.049	-0.006
A CO					
B Ni					
C $\text{CO}-\text{Ni}(\text{CO})$	0.487	0.217	2.24	-0.148	0.009
A CO					
B $\text{Ni}(\text{CO})$					
C $\text{CO}-\text{Ni}(\text{CO})_2$	0.446	0.209	2.13	-0.197	0.002
A CO					
B $\text{Ni}(\text{CO})_2$					
C $\text{CO}-\text{Ni}(\text{CO})_3$	0.442	0.209	2.11	-0.222	-0.011
A CO					
B $\text{Ni}(\text{CO})_3$					

of **2** and **3** and from the shift of the C–O stretching frequencies from **2** to **3**.

It is noteworthy that the carbodiphosphorane ligand $\text{C}(\text{PH}_3)_2$ is essentially a pure σ donor ligand in **2a** and at the same time stronger bonded than CO in $\text{Ni}(\text{CO})_4$, because $\text{M} \rightarrow \text{CO} \pi$ back-donation has been found as the dominant stabilizing contribution to the metal–carbonyl bonding.^{23a,45} However, recent theoretical work has shown that CO may also be strongly bonded to a transition metal when there is only negligible $\text{M} \rightarrow \text{CO} \pi$ back-donation.⁴⁶ The bonding properties of carbodiphosphorane in transition metal complexes may be compared with N-donor-stabilized carbenes, which are also essentially σ donor ligands with negligible π back-donation.^{47,48}

Theoretical Methods

The geometry optimizations and frequency calculations have been carried out at the DFT level using the three-parameter fit of the exchange–correlation potential suggested by Becke (B3LYP)³⁵ with our standard basis set II,³¹ which has an effective core potential (ECP)³⁶ with a (441/2111/41) valence basis set for Ni and 6-31G(d) all-electron basis sets for the first- and second-row atoms.³⁷ An ECP with a (31/31/1) valence basis set has been used for phosphorus.³⁸ The exponent for the d-type polarization functions is $\zeta(\text{P}) = 0.55$.³⁹ Single-point energy calculations at B3LYP/II optimized structures have been performed using coupled-cluster theory¹² with singles and doubles and noniterative estimation of triple excitations CCSD(T).¹³ The DFT calculations were performed with Gaussian 94.⁴⁰ For the CCSD(T) calculations the programs ACES II,⁴¹ Gaussian 94,⁴⁰ and Molpro⁴² have been employed. The nature of the stationary points was investigated by calculating

the Hessian matrices at the B3LYP/II level. All structures reported here are minima on the potential energy surface (number of imaginary frequencies $i = 0$) except $\text{Ni}(\text{CO})_2$. The energy minimum structure of nickel dicarbonyl at B3LYP/II has a bent geometry with a C–Ni–C angle of 151.3°, while the linear form is a transition state. However, CCSD(T)/II single-point energy calculations gave a lower energy for the linear form than for the bent structure. Therefore, we used the energy value of the linear form for the bond energy at CCSD(T)/II.

Inspection of the nickel–carbene interactions was carried out using the charge-decomposition analysis (CDA).¹⁵ In the CDA method the (canonical, natural, or Kohn–Sham) molecular orbitals of the complex are expressed in terms of the MOs of appropriately chosen fragments. In the present case, the Kohn–Sham orbitals of the B3LYP/II calculations are formed in the CDA procedure as a linear combination of the MOs of the $\text{C}(\text{PH}_3)_2$ or CO ligand and those of the remaining metal fragment NiL_n in the geometry of the complex. The orbital contributions are subdivided into four parts: (i) the mixing of the occupied MOs of the ligand and the unoccupied MOs of the metal fragment (donation ligand $\rightarrow \text{NiL}_n$); (ii) the mixing of the unoccupied MOs of the ligand and the occupied MOs of the metal fragment (back-donation $\text{L}_n\text{Ni} \rightarrow$ ligand); (iii) the mixing of the occupied MOs of the ligand and the occupied MOs of the metal fragment (repulsive polarization ligand $\leftrightarrow \text{NiL}_n$); and (iv) the residue term arising from the mixing of unoccupied orbitals. It has been shown that the residue term is ~ 0 for closed-shell interactions, while shared interactions have values for the residue terms that are significantly different from zero.^{16a–c} A more detailed presentation of the method and the interpretation of the results is given in refs 20 and 32. The CDA calculations have been performed using the program CDA 2.1.⁴³

Experimental Section

General Considerations. All operations were carried out under an argon atmosphere in dried and degassed solvents using Schlenk techniques. The IR spectra were run on a Nicolet spectrometer. ³¹P NMR spectra were recorded on a Bruker AC 300 instrument using 85% H_3PO_4 ($\delta = 0.00$ ppm) as the external standard. Elemental analyses were performed by the analytical service of the Fachbereich Chemie der Universität Marburg (Germany). $\text{Ph}_3\text{P}=\text{C}=\text{PPh}_3$ was prepared by a published method,⁹ improving the original procedure;⁴⁴ commercially available $\text{Ni}(\text{CO})_4$ was used without further purification.

Preparation of $(\text{CO})_3\text{NiC}(\text{PPh}_3)_2$ (2**).** The complex was prepared by slightly modifying the procedure described by Kaska.⁷ A solution of **1** (620 mg, 1.15 mmol) in 30 mL of toluene was treated with excess $\text{Ni}(\text{CO})_4$, and the mixture was stirred for 1 h at room temperature. A color change from yellow to yellow-orange occurred with gas evolution. The clear solution was layered with pentane and stored for several days at room temperature. Large orange crystals were separated from the mother liquor and dried in vacuum; yield 640 mg (82%), mp 124–126 °C dec. Anal. Calcd for $\text{C}_{40}\text{H}_{30}\text{NiO}_3\text{P}_2$: C 70.72, H 4.45. Found: C 70.90, H 4.52. IR (Nujol, cm^{-1}): $\nu(\text{CO})$ 2032, 1933. ³¹P NMR (400 MHz, THF): 9.92 ppm.

Preparation of $(\text{CO})_2\text{NiC}(\text{PPh}_3)_2$ (3**).** (a) From **1** and $\text{Ni}(\text{CO})_4$: The analogous procedure as described for **2** but in THF

as solvent gives a mixture of a few large crystals of **2** and deep red crystals of **3** which can be separated mechanically. (b) From **2**: Orange crystals of **2** (520 mg, 0.77 mmol) were dissolved in about 30 mL of THF, and the mixture was stirred for 24 h. The red solution was layered with pentane and stored for 3 days. Dark red crystals separated on the wall of the vessel and were collected and dried in a vacuum, mp 136–139 °C dec. Anal. Calcd for $C_{39}H_{30}NiO_2P_2$: C 71.92, H 4.64. Found: C 71.98, H 5.01. IR (Nujol, cm^{-1}): $\nu(CO)$ 1976, 1895. ^{31}P NMR (400 MHz, THF): 19.20 ppm.

Reaction of 2 with PPh_3 . A THF solution of **2** (680 mg, 1.18 mmol) was cooled to -78 °C. To the dark orange solution was added with stirring a slight excess of PPh_3 (360 mg 1.34 mmol). The solution immediately turned pale red and was pale yellow at room temperature. After filtration the solvent was removed in vacuo to give a yellow oily material. The IR spectrum of the oil showed three $\nu(CO)$ bands at 2068, 1998, and 1939 cm^{-1} , due to a mixture of $(CO)_2Ni(PPh_3)_2$ and $(CO)_3Ni(PPh_3)_2$. The ^{31}P NMR showed signals at 33.5, 31.9, and -3.9

ppm according to a mixture of $(CO)_2Ni(PPh_3)_2$, $(CO)_3Ni(PPh_3)_2$, and free **1**, respectively.

Acknowledgment. We thank the Deutsche Forschungsgemeinschaft (SFB 260 and Graduiertenkolleg Metallorganische Chemie) for financial support. Excellent service was provided by the computer centers HRZ Marburg, HLRZ Darmstadt, and HLRS Stuttgart. We are also grateful to the Fonds der Chemischen Industrie, Frankfurt/Main, Germany, and the Max-Planck-Society, Munich, Germany, for financial support.

Supporting Information Available: Tables of atomic positions, equivalent isotropic thermal parameters, and anisotropic thermal displacement coefficients (16 pages). Ordering information is given on any current masthead page.

OM9804632